Comparison of aftershock behavior of the flores sea 12 december 1992 and 14 december 2021

Adi Jufriansah[1], Azmi Khusnani[2], Yudhiakto Pramudya[3], Mulya Afriyanto[4]

[1,2]Department of Physics Education, IKIP Muhammadiyah Maumere, Jl. Jend. Sudirman, Waioti, Maumere, NTT

[3]Department of Master of Physics Education, Universitas Ahmad Dahlan, Jl. Pramuka, Umbulharjo, Yogyakarta, DIY

[4]Stasiun Meteorologi Fransiskus Xaverius Seda Sikka, Meteorological, Climatological, and Geophysical Agency, Jl. Angkasa Waioti, Maumere, NTT

E-mail: saompu@gmail.com

Received 17 February, Revised 24 March, Published 27 March 2023

Abstract: Over 30 years, the Flores region experienced earthquakes with Mw >7 twice, namely in 1992 and 2021 at shallow depths <60 km. However, the behavior of the aftershocks accompanying the quake has yet to be studied in detail. This research aims to compare the behavior of aftershocks after the main earthquake. This research uses three-lifetime analysis functions, namely, Wilber3, Mustang Web Browser, and comparison of Probability Density Function Hazard. The data used comes from IRIS data and BMKG Online Data. Through graphical analysis, it is known that the data for the time difference for aftershocks follow the RMS distribution, indicating that the Flores Sea aftershock on 12 December 1992 occurred with high intensity on the 3rd and the 6th day after the main earthquake. Meanwhile, the aftershocks in the Flores Sea on 14 December 2021 tended to occur with a more even intensity during the observation period, but the power returned to high on the 7th day.

Keywords: Aftershock, Wilber3, Mustang Web Browser, Probability DensityFunction Hazard, Flores Sea

1. Introduction

The physiographic data of Indonesia's territory is divided into three regional zones, including the Sunda Shelf, Sahul Shelf, and the Transitional Zone. The Sunda Shelf consists of the Java Sea, the Malacca Strait, and the South China Sea. The Sahul Shelf consists of the Aru Sea and the southern Banda Sea. Meanwhile, the transition zone consists of parts of the Banda Sea, Maluku Sea, Sulawesi Sea, and Flores Sea (Maimuna et al., 2022).

The Eurasian and Indo-Australian Plates traverse the Flores Sea with complex tectonic arrangements (Aslamia & Supardi, 2022). It is influenced by the subduction zone and the Mediterranean route with boundaries in the form of troughs, thus creating a seismic area with a relatively high frequency of seismicity (Miller & Zhang, 2021). Historically, several major earthquakes have been recorded in the Flores Sea. The earthquake catalog records for 30 years with magnitude Mw > 7, of which occurred in the Flores Sea in 1992 (Minoura et al., 1997; Handayani, 2019; Juliaus & Daryono, 2021; Felix et al., 2021; Polet & Kanamori, 2022), and the last recorded in 2021 (Hakim et al., 2022; Rohadi et al., 2022; Supendi et al., 2022). The complete condition of the large earthquake is presented in Figure 1.

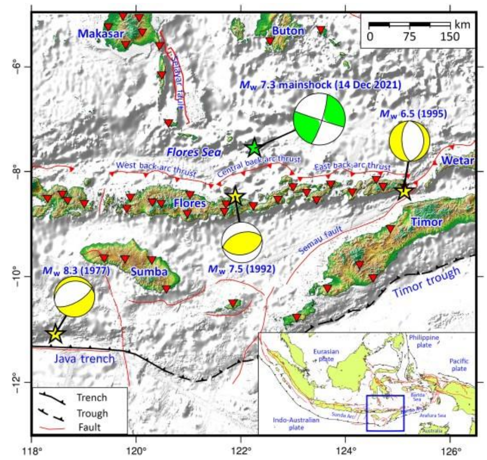

Figure 1. Mainshock of 12 December 1992 and 14 December 2021 (Supendi et al., 2022)

Several new findings have been obtained by seismotectonic experts, especially in the Eastern Indonesia region, that the rising fault segment, which was thought to be isolated from Flores Island and Wetar Island, was previously influenced by the Flores arc thrust (Supendi et al., 2020; Felix et al., 2022). It is acknowledged that this will expand the area along the boundary of the Java Sea strait from Alor Island to East Java in the Java Sea, which will cause significant earthquakes (Pranantyo et al., 2021). Rini et al. (2017) state that frequent large earthquakes are always followed by aftershocks (figure 2). This will appear within a certain period with different variations of earthquake attributes (DeVries et al., 2018; Jufriansah et al., 2021).

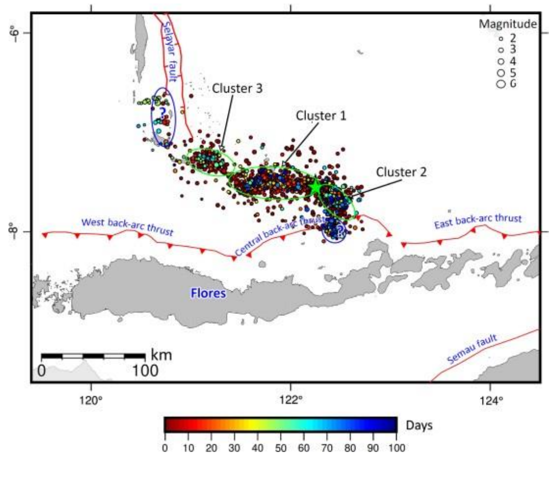

Figure 2. Aftershock events or aftershocks on December 14, 2021 presented in clusters. The color code shows the period of aftershock (Supendi et al., 2022)

Actively, the Earth plates of Timor, Sumba, and Flores began to collide with the Australian Continent starting from 9-10 Ma (Huang et al., 2000; Harris et al., 2009). As a result, there will be fewer moderate earthquakes (Mw ≥ 5.0) with a depth of <100 km. Other facts also state that there have never been shallow earthquakes (depth <100 km) with magnitude Mw ≥ 7.0 in the region from 1963 to 2021 (Hall, 2002; Keep & Haig, 2010; Ye et al., 2021; Rahman et al., 2021). Due to the structural complexity of the Banda Barat arc and lack of data, not all faults have been mapped correctly, including the one that ruptured and resulted on December 14, 2021. Therefore, to identify aftershocks due to the main earthquake by investigating the activity of the focal mechanism, this study aims to assess earthquake behavior follow-up Flores Sea 12 December 1992 and 14 December 2021.

2. Experimental

The data sources in this study used online data accessed through BMKG (Meteorology, Climatology, and Geophysics Agency) and IRIS (Incorporated Research Institution for Seismology). The seismic data used is aftershock data on December 12, 1992, and December 14, 2021, with a range of seven days after the main earthquake. The next step is to carry out the data acquisition process using Wilber3 with station data from the available networks, namely FDSN-ALL, GSN, and GFZ, with the location points according to figure 3.

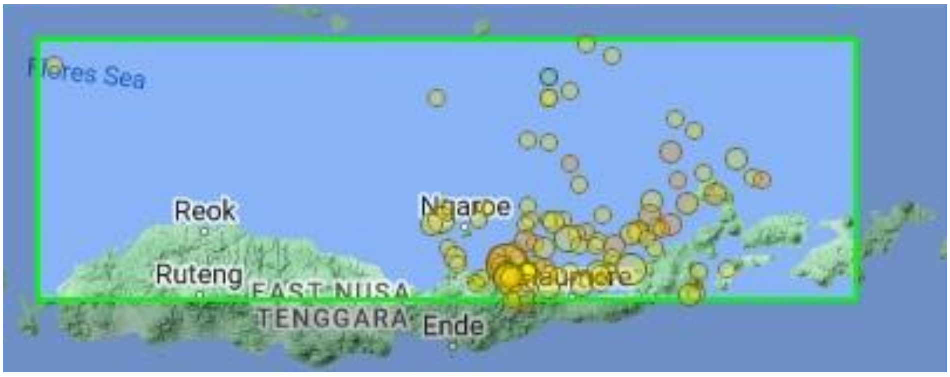

Figure 3. The location of the earthquake was taken 7 days after the main earthquake on 12 December 1992 (https://ds.iris.edu/wilber3/find_event)

The following process analyzes the data using Mustang, based on Wilber3 picking data to determine the RMS distribution as a comparison value for Probability Density Function Hazard. In total, the research flow is presented in Figure 4.

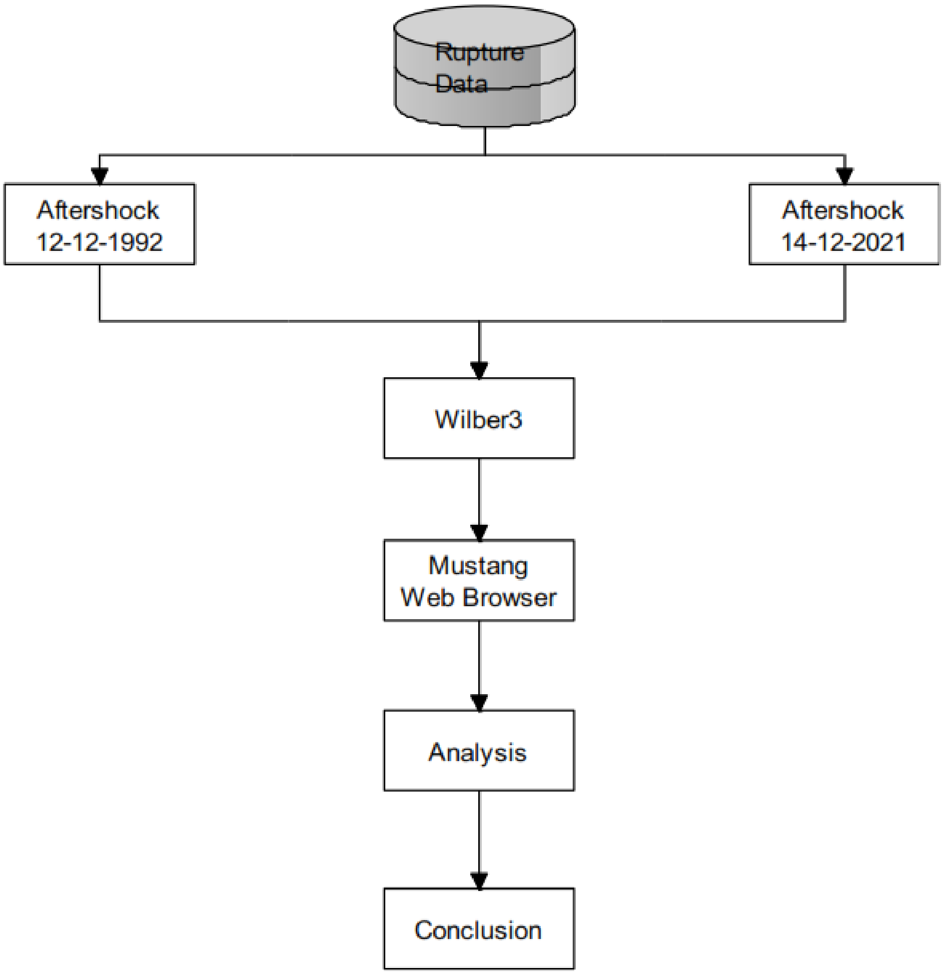

Figure 4. Research flow to analyze the aftershock of 12 December 1992 and 14 December 2021

3. Results and Discussion

Relocating the main earthquake on 12 December 1992 (figure 5) using the IRIS database with a minimum magnitude sorting value of Mw 3.0 obtained a total of 102 aftershocks, while the main earthquake on 14 December 2021 (figure 6) obtained 24 events. Reducing the total number of events minimizes the possibility of data noise resulting in errors in relocating events. It follows the BMKG catalog data regarding the initial location and selection of the time of arrival of sources, usually using a fixed depth for external events, which may be the reason for the inconsistency of the data obtained by the sensor (Supendi et al., 2022).

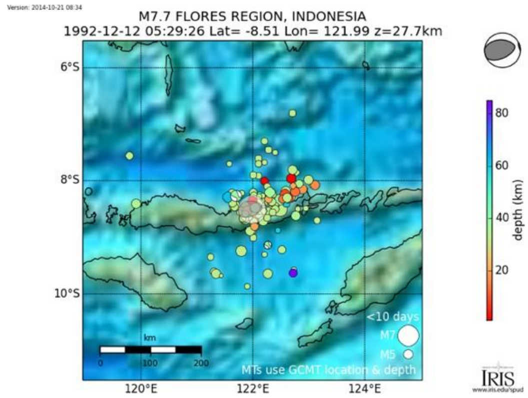

(a)

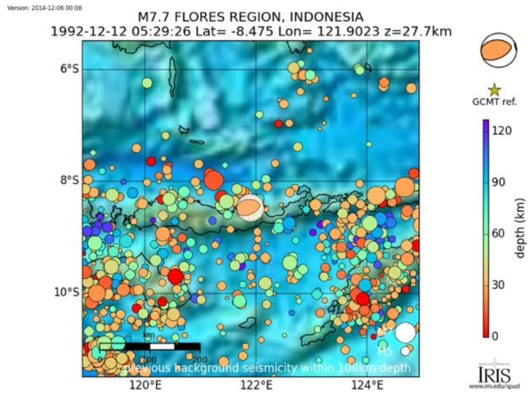

(b)

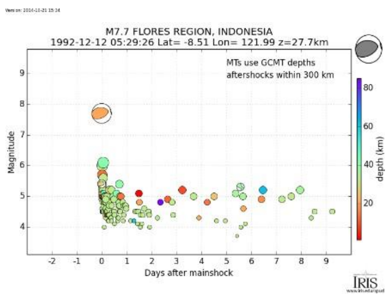

(c)

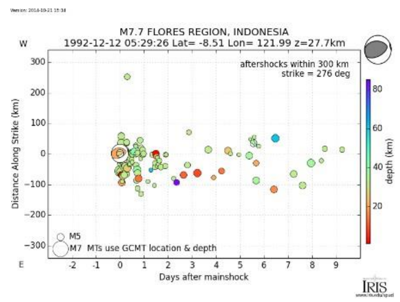

(d)

Figure 5. (a) December 12, 1992 aftershocks (b) Focal mechanisms GCMT ref (c) Days aftershock vs Magnitude (MTs use GCMT depths aftershock within 300 km) (d) Days aftershock vs Distance Along Strike (Aftershock within 300 km strike = 276 deg)

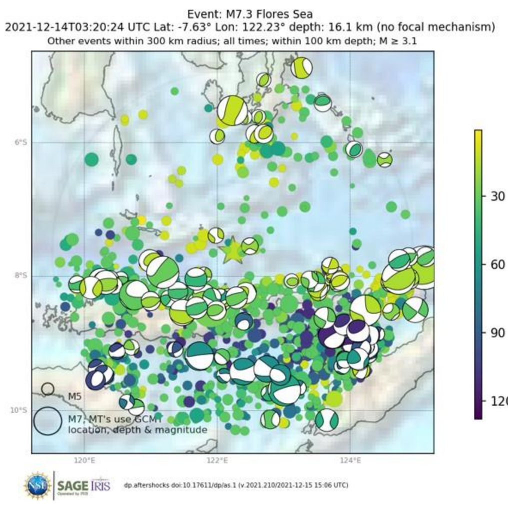

(a)

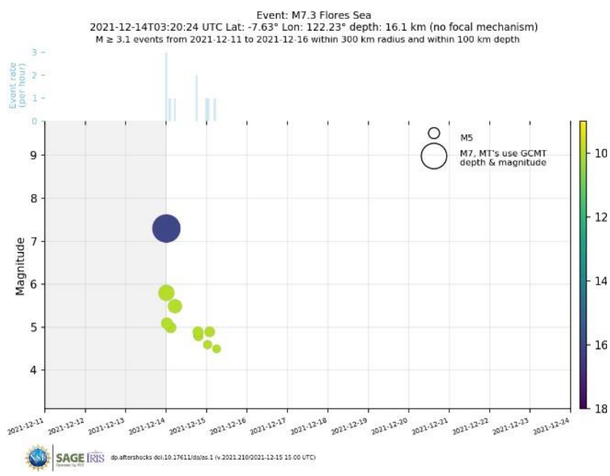

(b)

Figure 6. (a) Aftershock events December 14, 2021 (b) Days aftershock vs Magnitude (MTs use GCMT depths and magnitude)

The main Flores Sea earthquake of 12 December 1992 occurred along a seismically active part of the Indo-Australian plate. As reported by IRIS data, after the main earthquake with a distribution of magnitudes of aftershocks occurring in the range 4 ≤ Mw ≤ 6, while the Flores Sea aftershock on 14 December 2021, a distribution with an occurrence range of 4 ≤ Mw ≤ 5.8 was obtained. It shows an interesting pattern to study, especially the pattern of aftershocks resulting from the main Flores Sea earthquake on 14 December 2021. If the duration of the observation is extended to 20 March 2022, at least 3 clusters will be grouped. It is confirmed by Jufriansah et al. (2021) and Supendi et al. (2022) with the results obtained. Namely, the cluster 1 area is caused by the central east-west fault slip along 100 km, which is the location point of the Mw 7.3 earthquake. Cluster 2 triggers a southeast fault along 40 km to the east, while cluster 3 is oriented to the northwest along 50 km to the west. This analysis is then followed by a comparison of amplitude values using the probability density function hazard following the RMS distribution presented in Figure 7.

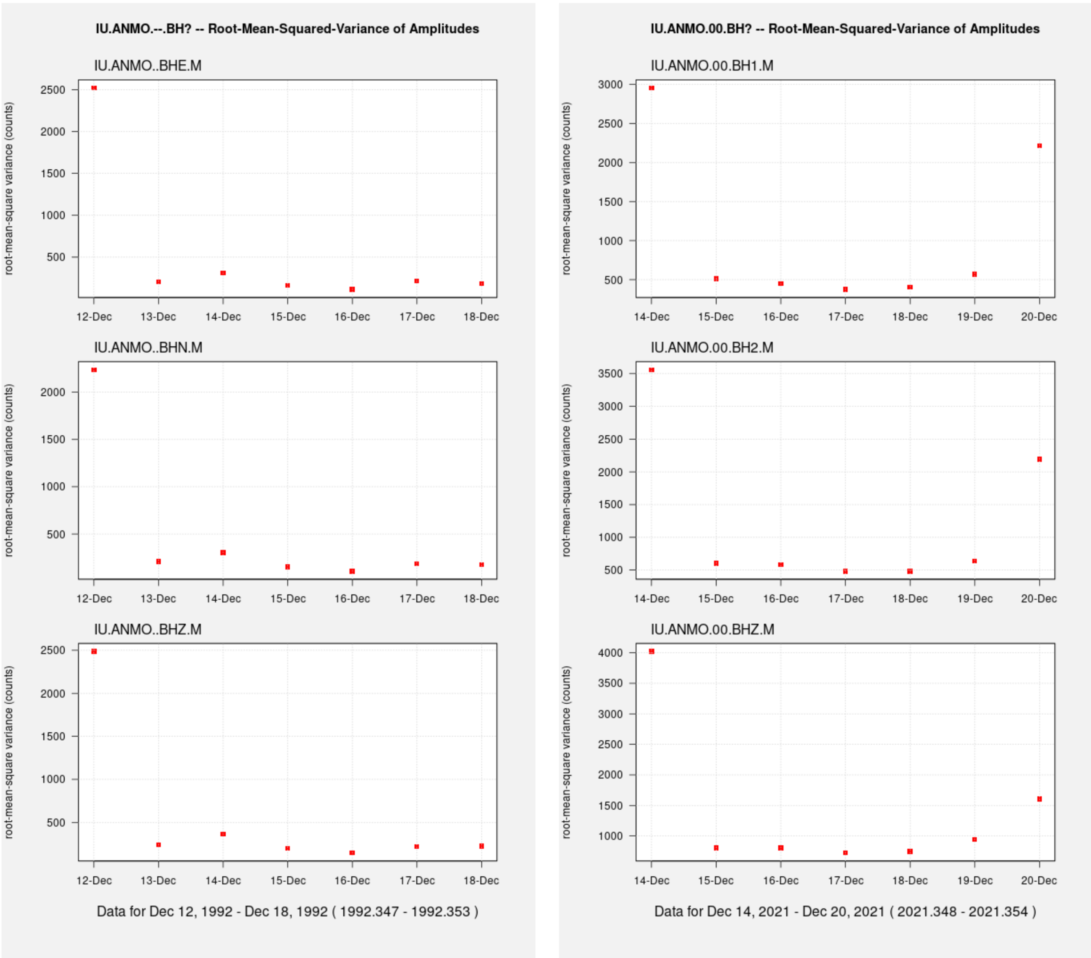

(a) (b)

Figure 7. The RMS distribution value is obtained by the Probability Spectral Density Function (a) Amplitude of the aftershocks of 12 December 1992; (b) Aftershock amplitude of 14 December 2021

Figure 7 is an analysis graph obtained from the aftershock time difference data following the RMS distribution using Mustang. These results indicate that the Flores Sea aftershocks on December 12, 1992, occurred with high intensity on the third and sixth day after the main earthquake with an amplitude variance value < 500. Meanwhile, the Flores Sea aftershocks on December 14, 2021, tended to occur with lower intensities. More evenly distributed during the observation period, but the intensity returned high on the seventh day with an amplitude variance value of > 1500. This finding was reinforced by Hakimi et al. (2022) that after aftershocks with a data length of one day (figure 8), there was an increase in amplitude on the sixth day. These results were obtained using the BMKG LRTI station.

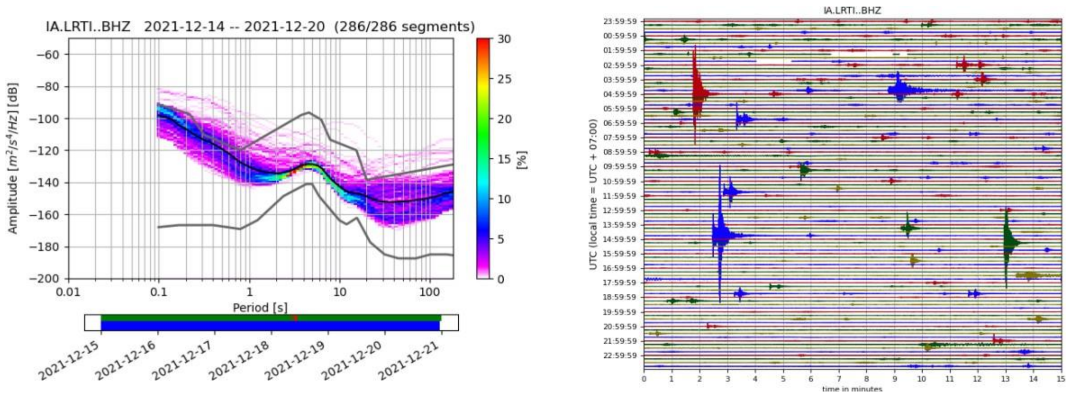

(a) (b)

Figure 8. Probability Spectral Density Function of aftershocks (a) Amplitudeaftershock (b) Noise seismogram (Hakim et al., 2022)

Shallow and deep earthquakes influenced the difference in the number of aftershocks observed. Several studies have discussed this (Page, 1968; Kagan & Knopoff, 1980; Frohlich, 1987). Only now much has yet to be discussed regarding aftershocks and the dangers they pose in the future (Zhang et al., 2020; Liu et al., 2022). Identifying and characterizing several substantial aftershocks still needs to be done to understand better (Wiens, 1998; Myers et al., 1995; Wu & Chen, 1999; Becker et al., 2019; Shen et al., 2019). A mainshock that occurs in a seismically active area will produce more aftershocks, with an average size similar to the mainshock compared to the aseismic area. However, this does not account for the difference in aftershock rates between deep and shallow earthquakes.

4. Conclusion

The results of comparing the aftershock behavior of the earthquakes on 12 December 1992 and 14 December 2021 have been obtained. These results were obtained based on the Wilber3 data acquisition process, followed by the graphical analysis method. It is known that the time difference for aftershocks follows the RMS distribution, indicating that aftershocks Flores 12 December 1992 occurred with high intensity on the third and sixth day after the main earthquake. While the aftershocks in the Flores Sea on 14 December 1992 tended to occur with a more even intensity during the observation period, the intensity returned to high on the seventh day. The aftershocks on the Flores Sea on 12 December 1992 with a distribution of magnitudes in the range of events 4 ≤ Mw ≤ 6, while the aftershocks in the Flores Sea on 14 December 2021 obtained the distribution of aftershocks in the range of events 4 ≤ Mw ≤ 5.8. These results are also strengthened based on comparisons of previous studies using the cluster method and probabilistic power spectral density.

Acknowledgements

We would like to thank LP3M IKIP Muhammadiyah Maumere for research funding.

References

Aslamia, H., & Supardi, Z. A. I. (2022). Analisis Parameter a-Value Dan b-Value sebagai Mitigasi Bencana Gempa Bumi di Nusa Tenggara Timur. Jambura Physics Journal, 4(1), 14-27.

Becker, J. S., Potter, S. H., McBride, S. K., Wein, A., Doyle, E. E. H., & Paton, D. (2019). When the earth doesn't stop shaking: How experiences over time influenced information needs, communication, and interpretation of aftershock information during the Canterbury Earthquake Sequence, New Zealand. International journal of disaster risk reduction, 34, 397-411.

DeVries, P. M., Viégas, F., Wattenberg, M., & Meade, B. J. (2018). Deep learning of aftershock patterns following large earthquakes. Nature, 560(7720), 632-634.

Felix, R. P., Hubbard, J. A., Bradley, K. E., Lythgoe, K. H., Li, L., & Switzer, A. D. (2022). Tsunami hazard in Lombok and Bali, Indonesia, due to the Flores back-arc thrust. Natural Hazards and Earth System Sciences, 22(5), 1665-1682.

Felix, R. P., Hubbard, J. A., Bradley, K., Lythgoe, K., Li, L., & Switzer, A. (2021). Tsunami hazard in Lombok & Bali, Indonesia, due to the Flores backarc thrust. Nat. Hazards Earth Syst. Sci. Discuss, 343, 1-26.

Frohlich, C. (1987). Aftershocks and temporal clustering of deep earthquakes. Journal of Geophysical Research: Solid Earth, 92(B13), 13944-13956.

Hakim, A. R., Saputro, A. H., Rohadi, S., Gunawan, M. T., & Kardoso, R. (2022, July). Seismic Noise Analysis in InaTEWS Earthquake Station Network (Case Study: Flores Earthquake 7.4, 14 December 2021). In IOP Conference Series: Earth and Environmental Science (Vol. 1047, No. 1, p. 012019). IOP Publishing.

Hall, R. (2002). Cenozoic geological and plate tectonic evolution of SE Asia and the SW Pacific: computer-based reconstructions, model and animations. Journal of Asian earth sciences, 20(4), 353-431.

Harris, R., Vorkink, M. W., Prasetyadi, C., Zobell, E., Roosmawati, N., & Apthorpe, M. (2009). Transition from subduction to arc-continent collision: Geologic and neotectonic evolution of Savu Island, Indonesia. Geosphere, 5(3), 152-171.

Huang, C. Y., Yuan, P. B., Lin, C. W., Wang, T. K., & Chang, C. P. (2000). Geodynamic processes of Taiwan arc–continent collision and comparison with analogs in Timor, Papua New Guinea, Urals and Corsica. Tectonophysics, 325(1-2), 1-21.

Jufriansah, A., Pramudya, Y., Khusnani, A., & Saputra, S. (2021). Analysis of Earthquake Activity in Indonesia by Clustering Method. J. Phys. Theor. Appl, 5(2), 92-103.

Julius, A. M., & Daryono, D. (2021). Overview of 1990s deadly tsunamis in Indonesia. In E3S Web of Conferences (Vol. 331, p. 07001). EDP Sciences.

Kagan, Y. Y., & Knopoff, L. (1980). Dependence of seismicity on depth. Bulletin of the Seismological Society of America, 70(5), 1811-1822.

Keep, M., & Haig, D. W. (2010). Deformation and exhumation in Timor: Distinct stages of a young orogeny. Tectonophysics, 483(1-2), 93-111.

L. Handayani, "Seismic Hazard Analysis of Maumere, Flores: a Review of The Earthquake Sources," Proceedings of the 7th Mathematics, Science, and Computer Science Education International Seminar, MSCEIS 2019, 12 October 2019, Bandung, West Java, Indonesia, 2020.

Liu, M., Li, H., Zhang, M., Wang, W., Yang, Y., Li, L., ... & Zhang, H. (2022). Investigation of the 2013 Eryuan, Yunnan, China MS 5.5 Earthquake Sequence: Aftershock Migration, Seismogenic Structure and Hazard Implication. Tectonophysics, 837, 229445.

Maimuna, A. K., Miftakhunnisa, A. F., & Segoro, Y. A. (2022). Pemodelan Inversi 3 Dimensi untuk Identifikasi Dugaan Keberadaan Sesar menggunakan Data Anomali Gaya Berat di Laut Flores (Studi Kasus Gempa Flores 14 Desember 2021). PROGRESS: Jurnal Geofisika, 1(1), 55-62.

Miller, M., & Zhang, P. (2021). Seismic Imaging of the Subducted Australian Continental Margin Beneath Timor and the Banda Arc Collision Zone.

Minoura, K., Imamura, F., Takahashi, T., & Shuto, N. (1997). Sequence of sedimentation processes caused by the 1992 Flores tsunami: evidence from Babi Island. Geology, 25(6), 523-526.

Myers, S. C., Wallace, T. C., Beck, S. L., Silver, P. G., Zandt, G., Vandecar, J., & Minaya, E. (1995). Implications of spatial and temporal development of the aftershock sequence for the Mw 8.3 June 9, 1994 deep Bolivian earthquake. Geophysical research letters, 22(16), 2269-2272.

Page, R. (1968). Focal depths of aftershocks. Journal of Geophysical Research, 73(12), 3897-3903.

Polet, J., & Kanamori, H. (2022). Tsunami earthquakes. Complexity in Tsunamis, Volcanoes, and their Hazards, 3-23.

Pranantyo, I. R., Heidarzadeh, M., & Cummins, P. R. (2021). Complex tsunami hazards in eastern Indonesia from seismic and non-seismic sources: Deterministic modelling based on historical and modern data. Geoscience Letters, 8(1), 1-16.

Rahman, Z., Rehman, K., Ali, W., Ali, A., Burton, P., Barkat, A., ... & Qadri, S. M. (2021). Re-appraisal of earthquake catalog in the Pamir—Hindu Kush region, emphasizing the early and modern instrumental earthquake events. Journal of Seismology, 25(6), 1461-1481.

Rini, L. S., Pratiwi, H., & Wiyono, S. B. (2017). Penerapan Model epidemic type aftershock sequence (ETAS) pada Data Gempa Bumi di Sumatra. URECOL, 281-286.

Rohadi, S., Azhar Prakoso, T., Yatimantoro, T., Rahman, A., Sunardi, B., Adimarta, A.,... & Karnawati, D. (2022, May). The 14 December 2021, Mw 7.4 Flores Earthquake: Review of the hypocenter relocation, slip distribution, coulomb stress, and seismic hazard. In EGU General Assembly Conference Abstracts (pp. EGU22-8366).

Shen, D., Zhang, Q., Xu, T., Zhu, H., Zhao, W., Yin, Z., ... & Xiong, H. (2019). Machine learning-enhanced realistic framework for real-time seismic monitoring—The winning solution of the 2017 international aftershock detection contest. Supendi, P., Nugraha, A. D., Widiyantoro, S., Pesicek, J. D., Thurber, C. H., Abdullah, C. I., ... & Rosalia, S. (2020). Relocated aftershocks and background seismicity in eastern Indonesia shed light on the 2018 Lombok and Palu earthquake sequences. Geophysical Journal International, 221(3), 1845-1855.

Supendi, P., Rawlinson, N., Prayitno, B. S., Widiyantoro, S., Simanjuntak, A., Palgunadi, K. H., ... & Arimuko, A. (2022). The Kalaotoa Fault: A Newly Identified Fault that Generated the M w 7.3 Flores Sea Earthquake. The Seismic Record, 2(3), 176-185.

Wiens, D. A. (1998). Source and aftershock properties of the 1996 Flores Sea deep earthquake. Geophysical research letters, 25(6), 781-784.

Wu, L. R., & Chen, W. P. (1999). Anomalous aftershocks of deep earthquakes in Mariana. Geophysical research letters, 26(13), 1977-1980.

Ye, L., Lay, T., & Kanamori, H. (2021). The 25 March 2020 MW 7.5 Paramushir, northern Kuril Islands earthquake and major (MW≥ 7.0) near-trench intraplate compressional faulting. Earth and Planetary Science Letters, 556, 116728.

Zhang, L., Werner, M. J., & Goda, K. (2020). Variability of ETAS Parameters in Global Subduction Zones and Applications to Mainshock–Aftershock Hazard AssessmentVariability of ETAS Parameters in Global Subduction Zones and Applications to Mainshock–Aftershock Hazard Assessment. Bulletin of the Seismological Society of America, 110(1), 191-212.